

Using an advanced simulation tool for successful conversion of reheating furnace to full oxyfuel operation

Esin Iplik* Tomas Ekman* Kristofer Bölke** Otto Kankaanpää***

*Linde Sverige AB, Varuvägen 2, 125 30 Älvsjö, Sweden (e-mail: esin.iplik@linde.com, tomas.ekman@linde.com).

**Linde Gas AB, Rättarvägen 3, 169 68 Solna, Sweden (e-mail: kristofer.bolke@linde.com)

***Ovako Imatra Oy AB, Terästehtaantie 1, 55610 Imatra, Finland (e-mail: otto.kankaanpaa@ovako.com)

Abstract: Oxyfuel combustion complements decarbonization efforts by reducing the energy needs in high-temperature industries. Steel reheating furnaces are good candidates for full oxyfuel operation since this can lead to up to 30% energy savings. Linde uses an in-house tool to simulate reheating furnaces for air-fuel to oxyfuel conversion. This paper follows a real customer case, starting with an airfuel simulation setup used to analyze the furnace, followed by oxyfuel simulations for burner design and energy savings estimations. These simulations lead to a successful installation of oxyfuel burners for the reheating furnace located at Ovako Imatra site. After the commissioning is completed, performance evaluation is done by comparing a reference airfuel operation period with an oxyfuel combustion period. Full oxyfuel conversion results in 27% energy savings for hot charge and high production rate periods thanks to significantly lower flue gas losses. Removing nitrogen from the oxidizer decreases the flue gas volume, reducing the total heat capacity of the off-gas stream. The savings are around 30% for cold charge and average production rate periods.

Keywords: oxyfuel combustion, energy savings, decarbonization, steel reheating.

1. INTRODUCTION

The decarbonization of electricity production, combined with increased electrification, has the potential to reduce the carbon footprint of low-temperature industries. However, high-temperature industries such as steel and glass production have a greater demand for heat that cannot currently be met without combustion. It is essential to develop efficient burner technologies to save energy and complement efforts to decarbonize fuel. One promising method is oxyfuel combustion, which uses industrial oxygen as an oxidizer to eliminate nitrogen from the gas mixture. This approach offers several benefits, including increased production capacity, reduced heat losses through flue gases, lower NO_x emissions, and lower CO₂ emission levels due to fuel savings. Research on oxyfuel combustion has been conducted for the steel industry (Hu et al., 2019) and the aluminum industry (Paubel et al., 2019).

Oxyfuel combustion has some inherent benefits. At a specific energy release, it creates low volumes of flue gas that has a higher fraction of highly radiating triatomic gas molecules. Any furnace designed for airfuel combustion can be fired more efficiently using oxygen as the oxidizer. The longer residence time of the highly radiating gases allows for a very efficient heat recuperation inside the furnace's dark zone. One potential drawback of traditional oxyfuel is the risk of forming high

amounts of NO_x due to the higher flame temperature. Linde has developed burners that overcome this problem by implementing semi-flameless and flameless combustion. The potential to efficiently supply more power than by using airfuel in any given furnace design also allows for the possibility to produce more if the material being heated allows for this.

Linde, with over 40 years of experience in oxyfuel combustion, is a trusted leader in the field. From studying lab-scale kinetics to converting large furnaces to 100% oxyfuel combustion, Linde has demonstrated its expertise. Reheating furnaces, being one of the most energy-demanding units in steel processing (Zhao et al., 2021), are excellent candidates for oxyfuel conversion. These furnaces, used to reheat blooms or billets to the rolling temperatures of around 1150 - 1300 °C, constitute up to 67% of the total steel energy demand (Vögele et al., 2020).

Ovako Group has been active in their decarbonization efforts since 1995 by switching reheating furnaces (Hofors, Sweden) into oxyfuel combustion as well as High-Level Lancing (HLL) of oxygen at other Ovako locations (Smedjebacken and Hällefors, Sweden). The following efforts included electrification of heat treatment furnaces and electrolyzer investments to use fossil-free hydrogen for combustion. This paper follows the conversion of Ovako Imatra's reheating furnace to full oxyfuel operation using simulations and real data for airfuel vs. oxyfuel comparisons regarding energy savings and capacity increase. These numerical simulations

allow a better understanding and an optimal design of the oxyfuel combustion system. Additionally, they predict the furnace performance with the suggested changes ensuring a more confident project execution.

Another installation of oxyfuel technology is planned at their Boxholm plant in Sweden. The Imatra plant in Finland is making a major effort to decarbonize Ovako's steel production, and the conversion of the bloom furnace is the first major leap. The converted furnace, the first large-scale reheating furnace in Finland using solely flameless oxyfuel technology, is a testament to the potential of oxyfuel conversion. This successful conversion not only enables the use of hydrogen as a fuel, but also allows Ovako's to move towards its goal of zero-carbon production.

Conversion to full oxyfuel lowers the total flue gas volume and can cause difficulties in furnace pressure control depending on the flue gas system sizing. Maintaining the furnace pressure is essential to prevent air ingress, and slight positive pressure is preferred for industrial furnaces. Therefore, some furnaces may have a minimum power limitation to generate enough flue gas volume. The flue gas system is often redesigned during the conversion, and the furnace pressure control damper is rebuilt. The target furnace of this work is a walking beam furnace used to heat blooms. During airfuel operation, it had roof-mounted burners for the top zones and lateral burners for the bottom zones. For oxyfuel operation, the roof burners are repositioned as lateral burners. The baffles between the recuperative and fired bottom zones were removed to accommodate two additional fired zones. No other major modifications were made. The furnace has an installed economizer in the stack, and it is kept in use after the oxyfuel conversion despite not using the hot combustion air anymore. Heat recovered by the economizer, as well as from cooling of walking beams, is used in district heating around the mill. The furnace pacing system stayed unchanged, and the heating control system was adapted to new zones and gas compositions.

2. METHODOLOGY

The simulation code used for this work is based on the blooms being evenly spaced in the furnace with no empty spaces. Even pacing of blooms is assumed for transportation through the furnace. One target condition is uniform temperature distribution within the material with less than 30 °C gradient between 10% under the top surface and the center of the bloom when it exits the furnace. Reference thermocouple measurements are taken from the furnace zones. The temperature-dependent emissivity of the furnace walls and the heated material are selected as inputs, as well as the chemical composition of the reference alloy. The model calculates the fired zone temperatures and the power used in the fired zones to achieve the material target temperatures at the selected production rate.

The furnace model is divided into zones that can be used for heating or recuperation. While heating zones are fired, recuperation zones are not. These zones are adapted to the customer furnace and correspond to the control strategy. The furnace is, then, subdivided into computational cells, as shown in Fig. 1. Each cell has two energy balances that must be fulfilled, one on the cell wall and one for the gas volume in the cell. The cell is assumed to be an ideal continuous stirred-tank

reactor, and the cell models include the radiation and convection energy fluxes from gas to wall, gas to material, wall to material, wall to surroundings, and cell to cell. The gas radiation is evaluated according to the method described in VDI-Wärmeatlas section KC (Stephan et al., 2021). The standard view factor methods compute the wall and material surface radiative interactions (Stephan et al., 2021). Convection constitutes a minor part of the heat transfer and uses the Juerges' standard forced convection equation (Mörtstedt and Hellsten, 1994). The simulation code sets up a system of differential equations based on the number of cells. The solver uses two input parameters for each cell and solves the equation system by finding the correct gas temperature or power input with wall temperatures that satisfies the set of equations with a minimum error.

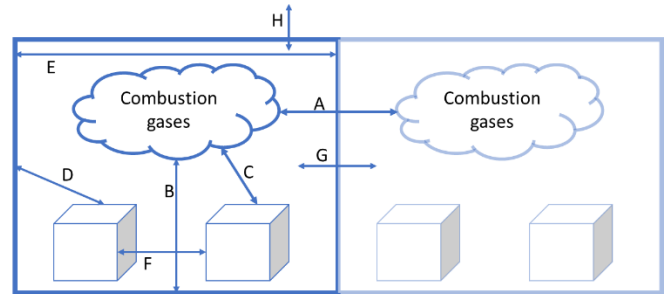


Fig. 1. Energy fluxes considered. (A: Gas to gas, B: Gas to wall, C: Gas to material, D: Wall to material, E: Wall to wall, F: Material to material, G: Cell to cell, H: Wall to surroundings.)

The material pieces are also divided into computational nodes, and the transient response of the nodes is calculated by the very efficient Thomas algorithm, modified to use non-constant material properties (Lee, 2024).

The solver generates a steady-state solution to the particular problem setup. This solution highly depends on the temperature status of all the material surfaces in the furnace. To generate this solution, the transient response of the material transported through the furnace is recalculated many times during the solution procedure. The KINSOL solver (<https://computing.llnl.gov/projects/sundials>), with Broyden root finder (Broyden, 1965), is used for the simulation.

For the Ovako Imatra case, 0.5 m furnace cells were selected, which generated 37 cells for both the top and bottom zones. This setup created 148 energy balance equations to be solved simultaneously. For computational efficiency and desired accuracy, the material node was selected to be 39 x 46 mm. The selected material dimensions were 310 x 370 x 4400 mm.

Linde and Ovako agreed on the following simulation scenarios for airfuel vs. oxyfuel comparison.

- Scenario 1: Cold charged blooms, 20 °C, 38 tph pace, ~4 hours in the furnace with target temperature of ~1250 °C
- Scenario 2: Hot charged blooms, 800 °C surface temperature, 900 °C core temperature, 75 tph pace, ~2 hours in the furnace with target temperature of 1250 °C

These simulations represent ideal production scenarios; however, the reality is usually non-ideal. The production follows the demand. Therefore, material size, characteristics,

and heating requirements change during continuous operation. It is hard to simulate the real furnace, considering the temperature, power, and production rate changes. Ideal scenarios are used to demonstrate the differences between airfuel and oxyfuel operations.

Before oxyfuel conversion, airfuel data is collected from the furnace, including fuel flow, bloom charge and discharge temperature, and production rate. Data is collected during a week and classified according to charge temperature to evaluate the energy requirements separately. The reference airfuel simulation is forced to match the reference airfuel data, and the furnace losses are calculated according to the energy balances. These losses are kept constant and used for the oxyfuel simulation to represent the furnace as close as possible to reality without expecting furnace improvements.

Data sets are described below.

- Data set 1: Cold charged blooms, below 100 °C, above 25 t/h
- Data set 2: Hot charged blooms, over 800 °C, above 55 t/h
- Data set 3: Hot charged blooms, over 800 °C, all production rates
- Data set 4: Mixed temperature charges, between 100 and 800 °C, all production rates

After the oxyfuel installation, performance evaluation data is collected for one week. Oxyfuel data is also classified as described above for comparison.

Data sets 1 and 2 are similar to the simulation scenarios; however, values differ slightly due to the very limited number of data points that satisfy the simulation conditions.

3. SIMULATION RESULTS

Linde creates simulations during the project evaluation period using furnace design, burner equipment, fuel selection, material heating requirements, fuel consumption, production rate, combustion air temperatures, and material grade information supplied by Ovako.

An image of the simulation interface for airfuel operation is given in Fig. 2. The fired top and bottom zones and flue gas flow direction are shown in this figure, in addition to the thermocouple locations. Material flows opposite the flue gas flow (pink arrows) direction. The furnace starts with two recuperation zones (left-hand side), followed by six fired zones (three top and three bottom). The off-gas duct is marked with red arrows, and potential air leakage is marked with blue arrows. Fired zones are shown with the yellow flame, and the thermometer indicates the location of the thermocouples.

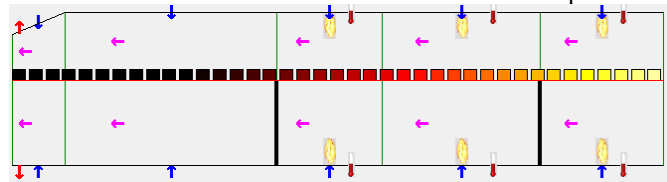


Fig. 2. Airfuel simulation setup.

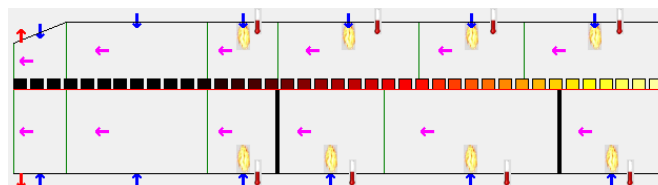


Fig. 3. Oxyfuel simulation setup.

Oxyfuel simulation presents the availability for two additional fired zones thanks to efficient recuperation of the heat in the low flue gas volume. As shown in Fig. 3, one top and one bottom fired zone are added to the furnace, shortening the recuperation zone to start heating the blooms earlier and allowing the material to distribute the heat for a longer time.

Table 1 shows the operating parameters and the resulting energy consumption. The solver is restricted by the maximum allowed wall temperature, available installed power, and the temperature homogeneity requirements of the blooms at discharge. Simulation results are reasonable with respect to the acquired furnace data.

Table 1. Airfuel simulation results as reference points.

Case	Charge T (°C)	Discharge T (°C)	Production rate (t/h)	Energy Consumption (kWh/t)
Sc. 1	20	1250	38	334
Sc. 2	800	1250	75	144

To achieve the target temperatures with oxyfuel installation, simulations are reset, and new power values are estimated using oxyfuel burners. The results of these simulations are used to calculate energy savings, as summarized in Table 2.

Table 2. Results of the oxyfuel furnace simulations.

Case	Charge T (°C)	Discharge T (°C)	Production rate (t/h)	Energy Consumption (kWh/t)
Sc. 1	20	1250	38	296
Sc. 2	800	1250	75	119

Based on the simulations, an 11% improvement is calculated for cold charging (Sc. 1), and a 17% improvement is expected for hot charging at high production rates (Sc. 2). Based on these simulations, Linde and Ovako agreed on full oxyfuel conversion of the selected furnace.

4. PERFORMANCE EVALUATION

Performance comparison is based on the data obtained during the reference period prior to the oxyfuel installation and from a total production week using oxyfuel after the commissioning. Energy usage data is logged as hourly totals. For each hour, the number of tons of product discharged is evaluated to represent the production rate. The charge and discharge temperatures are averages of all the blooms extracted during the hour. Selected hours are consecutive in time to reflect continuous production and charging of blooms.

Table 3. Airfuel reference data.

Case	Charge T (°C)	Discharge T (°C)	Average Production Rate (t/h)	Energy Consumption (kWh/t)
Set1	41	1234	40	373
Set2	849	1212	62	170
Set3	835	1212	42	333
Set4	576	1220	38	366

Reference data from the airfuel operation is given in Table 3. The data shows the highest energy consumption for the cold-charged blooms, as expected, represented as Set1. The simulation results given in Table 1 and Table 2 represent a fully continuous production. On the other hand, the actual scenarios in Table 3 and Table 4 are averages of hours with higher and lower production rates, possibly including minor stops between changing production parameters. It can be expected that the actual production has a higher energy consumption than the simulation. This explains the deviation between the simulation setups and the real data for both hot and cold-charged scenarios. Furthermore, Set2 has a significantly lower average production rate than the simulation, which also contributes to higher energy consumption than the simulation.

Set3 and Set4 are not simulated but are used for performance evaluation. Set4 is a mix of higher and lower charge temperatures, and the energy consumption value lies between the cold (Set1) and the hot charge (Set3). As expected, and simulated, higher charge temperatures require lower energy consumption per ton of product to reach the target discharge temperature. Changing the production rate affects consumption significantly. The subset taken from Set3 is given as Set2, which includes only the highest production rates. The lowest energy consumption is achieved during these high throughput hours. This high efficiency has an upper limit defined by the combustion system, furnace design, charge material, and production requirements.

The target furnace is converted to full oxyfuel operation by Linde according to the simulations with the additional fired zones. Oxyfuel-fired burners are shown in Fig. 4. After the commissioning, some blooms are charged with

thermoelements installed on them to measure the temperature distribution in the material, as shown in Fig. 5.



Fig. 4. Oxyfuel burners as installed with heated bloom in the foreground.



Fig. 5. Bloom with thermoelements being discharged from the furnace.

The oxyfuel performance data is presented in Table 4.

Table 4: Oxyfuel performance data.

Case	Charge T (°C)	Discharge T (°C)	Average Production Rate (t/h)	Energy Consumption (kWh/t)
Set1	14	1247	36	261
Set2	871	1236	61	123
Set3	830	1244	43	163
Set4	622	1237	33	241

Oxyfuel and airfuel follow the same trend for all the scenarios. As expected, oxyfuel energy consumption is consistently lower than airfuel. The highest energy consumption belongs to the cold-charged material (Set1). Despite a 10% lower production rate, 25 °C lower average charge temperature, and 10 °C higher discharge temperature of oxyfuel operation, energy savings of 30% are achieved for cold-charged blooms reheating. Simulation setup 1 represents a similar case to Set1. The simulation shows an improvement of only 11% in terms

of energy savings. As explained earlier, this value does not account for any furnace improvements. However, extensive commissioning maintenance carried out during the oxyfuel installation at the Imatra site should contribute to this deviation, together with the inherent ability of oxyfuel systems to quickly adapt to varying production scenarios. Oxyfuel systems are more agile than airfuel systems due to their higher heat transfer capability. Furnaces with varying production rates benefit oxyfuel combustion greatly. It shall also be noted that the simulation software is designed to be slightly conservative in its estimations of oxyfuel performance so as not to promise excessive energy savings.

A considerable 27% energy saving is achieved by oxyfuel conversion for the high production rates of the hot-charged material (Set2). For hot charging, the high flue gas temperatures penalize airfuel systems more than oxyfuel systems due to the high flue gas volume of airfuel combustion. Simulation setup 2 represents this scenario best, and it estimated an improvement of 17%, which is lower than the actual performance improvement of 27%. This deviation can be explained by the same reasons described above. Additionally, the average charge temperature of the oxyfuel Set2 is 20 °C higher than the airfuel case.

The highest energy savings are observed for the hot charge in Set3, at 51%. While the charge temperature and production rates are comparable for airfuel and oxyfuel Set3, the oxyfuel combustion data set has a 30 °C higher average discharge temperature. The possible explanation for the very high energy savings, in addition to the aforementioned furnace maintenance, is likely the higher variance in the production rates for the airfuel reference period compared to the oxyfuel period.

Set4, with the mixed charge temperatures, shows a 34% improvement after the oxyfuel conversion. Oxyfuel data has the advantage of receiving a higher-temperature charge. However, it also has a higher discharge temperature and a lower average production rate, balancing the comparison.

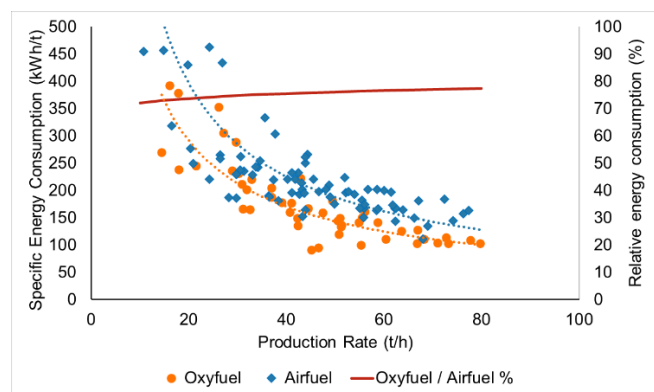


Fig. 6. Performance evaluation data for hot charge.

The hourly performance evaluation data for hot charge is plotted against the production rate for both airfuel and oxyfuel reference periods, given in Fig. 6. Percent improvement is plotted based on the trendlines. The benefit of oxyfuel slightly increases with the increasing production rate. If the airfuel-

fired furnace is run at a much higher production rate, the furnace efficiency will drop. This effect can be seen in Fig. 6. At rates above 70 t/h, all data points are found above the trendline that best fits the data set.

Based on the overall performance evaluation data, total energy savings for the reference period are estimated at 43%. It is worth mentioning that the economizer and cooling water heat recovery gains are not included in the efficiency calculations of oxyfuel operation, which translates to a further 10% savings of the total supplied energy.

5. CONCLUSIONS

Oxyfuel combustion is an efficient method to save energy in steel reheating furnaces. Increasing the heat transfer capacity and lowering the flue gas volume, hence the energy loss to the atmosphere, these systems have a proven track record of achieving higher performance against traditional airfuel combustion. This work shows both simulation and performance evaluation of oxyfuel and airfuel combustion at Ovako Imatra blooms reheating furnace. The simulation scenario showing a 17% improvement for high production rates of hot-charged material is supported by the real data showing a 27% improvement after complete oxyfuel conversion. Finally, 43% energy savings is achieved during the reference oxyfuel evaluation period.

REFERENCES

- Broyden, C. G. (1965). Class of Methods for Solving Nonlinear Simultaneous Equations. *Mathematics of Computation*, 577 - 593.
- Hu, Y., Tan, C., Niska, J., Chowdhury, J. I., Balta-Ozkan, N., Varga, L., Roach, P. A., and Wang, C. (2019). Modelling and simulation of steel reheating processes under oxy-fuel combustion conditions - Technical and environmental perspectives. *Energy*, 730-743.
- Lee, W. (Retrieved July 12, 2024). *Tridiagonal matrices: Thomas Algorithm*. Retrieved from <http://www.industrial-maths.com/>
- Mörtstedt, S.-E., Hellsten, G. (1994). *Data och diagram*. Stockholm: Liber Utbildning.
- Paubel, X., Rheker, F., Juma, S., Jepson, S., Wieck, and D., Ollerton, B. (2019). Oxy-fuel Technologies for Improved Efficiency in Aluminum Scrap Melting. *Light Metals* (págs. 1165-1172). San Antonio: Springer.
- Stephan, P., Kabelac, S., Kind, M., Mewes, D., Schaber, K., and Wetzel, T. (2021). *VDI-Wärmeatlas*. Berlin: Springer.
- Vögele, S., Grajewski, M., Govorukha, K., and Rubbelke, D. (2020). Challenges for the European steel industry: Analysis, possible consequences and impacts on sustainable development. *Applied Energy*, 114633.
- Zhao, J., Ma, L., Zayed, M. E., Elsheikh, A. H., Li, W., Yan, Q., and Wang, J. (2021). Industrial reheating furnaces: A review of energy efficiency assessments, waste heat recovery potentials, heating process characteristics and perspectives for steel industry. *Process Safety and Environmental Protection*, 1209-1228.